



Vapor phase hydrofluorination of acetylene to vinyl fluoride over $\text{La}_2\text{O}_3\text{-Al}_2\text{O}_3$ catalysts

Qing-Yuan Bi^a, Lin Qian^a, Li-Qiong Xing^a, Li-Ping Tao^a, Qiang Zhou^b, Ji-Qing Lu^a, Meng-Fei Luo^{a,*}

^a Zhejiang Key Laboratory for Reactive Chemistry on Solid Surfaces, Institute of Physical Chemistry, Zhejiang Normal University, Jinhua 321004, China

^b Juhua Group Engineering Technology Research Center of National fluoride materials, Quzhou 324004, China

ARTICLE INFO

Article history:

Received 11 January 2009

Received in revised form 2 March 2009

Accepted 2 March 2009

Available online 14 March 2009

Keywords:

Hydrofluorination

Vinyl fluoride

$\text{La}_2\text{O}_3\text{-Al}_2\text{O}_3$ catalyst

Coke deposition

Acidic sites

ABSTRACT

A series of La-doped Al_2O_3 catalysts were prepared and tested for the vapor phase hydrofluorination of C_2H_2 to vinyl fluoride (CH_2CHF , VF). It was found that the La-doped catalyst gave a stable catalytic performance and a higher selectivity to the desired VF and a lower selectivity to coke deposition compared with the pure Al_2O_3 catalyst. The enhancement in VF selectivity on the La-doped catalyst was due to the elimination of acidic sites on the Al_2O_3 surface by the addition of La_2O_3 , evidenced by NH_3 -TPD results, which could also explain the declined selectivity to coke deposition on the catalyst. Raman result indicated there were two different vibration forms of C–H distortion and C=C expansion for the coke deposition.

Crown Copyright © 2009 Published by Elsevier B.V. All rights reserved.

1. Introduction

It is well known that vinyl fluoride (VF) is an important fluorine-containing monomer, which is usually used to synthesize poly-vinyl fluoride (PVF), fluoropolymers and other fluorine-containing fine chemicals. Because PVF has many advantages such as being resistant to weather, good mechanical strength, chemical inertness, and low permeability to air and water, it has broad applications and thus attracts much attention in its synthesis.

At present, the main processes of VF synthesis are listed as follows [1–4]:



Considering the atomic efficiency and environmental issue, reaction (4) is obviously much preferred. The catalysts used in this reaction mainly include Hg-containing, Cd-containing, Cr-containing, CuCN, fluorine sulfonic acid and metal chloride compounds. But these compounds are limited in application due to their strong toxicity [5,6]. An alternative Al_2O_3 catalyst gives a high C_2H_2

conversion and high selectivity to VF for vapor phase hydrofluorination of C_2H_2 . However, since the Al_2O_3 catalyst has strong acidity, it suffers severe deactivation because of the coke deposition on the catalyst surface during the reaction [6,7], particularly for the molecules with high C/H molar ratio [8], such as alkyne hydrocarbon.

To restrain the coke deposition, alkali metals (K, Na) oxide and/or alkaline-earth metals (Mg, Ca) oxides were added in the Al_2O_3 , to modify the surface acidity of catalyst [9–11]. Besides, rare-earth metals are also effective in reducing the coke deposition [12]. For instance, La_2O_3 can enhance the stability of Al_2O_3 catalyst for carbon dioxide reforming of methane [13], CO_2 reforming of methane to syngas [14] and catalytic combustion of methane [15].

Budi et al. [16] reported that the presence of La on the surface of zeolite improved the stability of Cu-ZSM-5 catalyst by reducing the degree of the copper migration to the external surface of the catalyst. Also, La can stabilize $\gamma\text{-Al}_2\text{O}_3$ and enhance its stability for many reactions, as reported in the literature [17–23].

In this work, La-doped Al_2O_3 catalysts were employed in the vapor phase hydrofluorination of C_2H_2 . The effect of La doping on the catalytic property of the catalyst was studied.

2. Results and discussion

2.1. Influence of reaction temperature and $\text{HF}/\text{C}_2\text{H}_2$ molar ratio

Fig. 1 shows the C_2H_2 conversion, selectivities to the main products and coke deposition at different reaction temperatures

* Corresponding author. Tel.: +86 579 82282234; fax: +86 579 82282595.
E-mail address: mengfeiluo@zjnu.cn (M.-F. Luo).

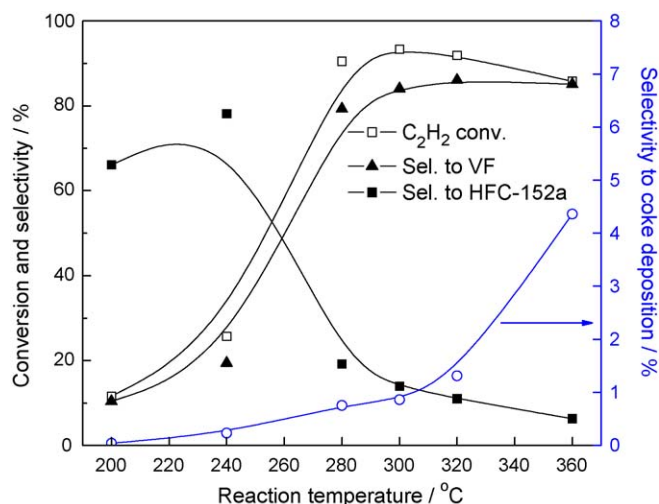


Fig. 1. C_2H_2 conversion, selectivities to the main products and coke deposition at different reaction temperatures on $La_2O_3(1)-Al_2O_3$ catalyst.

over the $La_2O_3(1)-Al_2O_3$ catalyst. It is a typical profile in the $La_2O_3-Al_2O_3$ system studied in the current work. The selectivities to other unknown and minor products were not discussed in this work. It can be seen that with increasing reaction temperature, the C_2H_2 conversion increases until it gets to a maximum at about 300 °C and then declines slowly. More interestingly, the highest selectivity to VF (84.1%) is also obtained at around 300 °C and it keeps at this level at higher reaction temperature. Meanwhile, the selectivity to the by-product 1,1-difluoroethane (CHF_2CH_3 , HFC-152a) is approximately 78.2% at 240 °C, but it quickly declines with increasing temperature, with a selectivity of 14.9% at 300 °C. The decline in the selectivity to HFC-152a is due to the fact that HFC-152a could be decomposed to VF (reaction (3)) at high temperature. As for the coke deposition, when the reaction temperature is lower than 300 °C, its selectivity is quite low (ca. 0.9%). However, when the temperature rises higher than 300 °C, it increases quickly. This is due to the enhanced conversion of C_2H_2 , accompanied by an increasing formation rate of ethylene, which could strongly adsorb on the catalyst surface and consequently form coke deposition. Taking into account of these aspects, we think that the reaction temperature of 300 °C is appropriate for the VF synthesis; therefore it is chosen for the rest of the investigation.

Table 1 lists the influence of HF/ C_2H_2 molar ratio on the reaction over the $La_2O_3(1)-Al_2O_3$ catalyst. As can be seen in Table 1, the C_2H_2 conversion, VF and HFC-152a selectivities can be modified by changing the HF/ C_2H_2 molar ratio. The C_2H_2 conversion increases with increasing HF/ C_2H_2 molar ratio, however, the selectivity to VF declines and the selectivity to HFC-152a increases. This is due to the accelerated formation of HFC-152a, resulting from the further reaction of VF with HF at a higher content of HF in the feed gas. It is interesting that the selectivity to coke deposition hardly changes, indicating that the increasing concentration of HF in the feedstock

Table 1

Influence of HF/ C_2H_2 molar ratio on catalytic performance.^a

HF/ C_2H_2 ratio	C_2H_2 conversion (%)	Selectivity (%)		
		VF	HFC-152a	Coke deposition
1.5	69.7	95.5	2.8	0.8
2.5	94.5	84.1	14.9	0.9
3.5	97.8	70.5	28.3	1.0
5.0	99.0	55.0	43.8	1.0
6.0	99.1	49.0	49.3	1.0

^a Catalyst: $La_2O_3(1)-Al_2O_3$. Reaction temperature: 300 °C.

Table 2

Influence of La content on catalytic behavior of $La_2O_3-Al_2O_3$ catalysts for hydrofluorination of C_2H_2 to VF.^a

La content (mol%)	C_2H_2 conversion (%)	Selectivity (%)		
		VF	HFC-152a	Coke deposition
0	96.1	78.4	19.0	2.1
1	94.5	84.1	13.9	0.9
5	92.4	81.1	16.4	0.8
10	88.0	83.3	15.6	0.8

^a Reaction temperature: 300 °C.

exerts little function on it. Also, when the HF/ C_2H_2 molar ratio exceeds 2.5, the conversion of C_2H_2 hardly changes, due to the fact that the stoichiometric ratio HF/ C_2H_2 needed for the reactions (C_2H_2 to VF and VF to HFC-152a) is 2.

2.2. Influence of La content in the $La_2O_3-Al_2O_3$ catalyst

Table 2 lists the influence of La content on catalytic behavior of $La_2O_3-Al_2O_3$ catalysts. It shows that the selectivity to VF is enhanced considerably from 78.4% over the Al_2O_3 catalyst to 84.1% over the $La_2O_3(10)-Al_2O_3$ catalyst, and the selectivity to coke deposition decreases from 2.1 to 0.9% with increasing La content. However, the conversion of C_2H_2 declines slightly from 96.1% over the pure Al_2O_3 catalyst to 88.0% over the $La_2O_3(10)-Al_2O_3$ catalyst. Among the $La_2O_3-Al_2O_3$ catalysts, the $La_2O_3(1)-Al_2O_3$ catalyst gives very high C_2H_2 conversion (94.5%) and the highest VF selectivity (84.1%). In order to intrinsically compare the catalytic performance of these catalysts, Table 3 lists the influence of La content on the products selectivities at the 90% of C_2H_2 conversion over $La_2O_3-Al_2O_3$ catalysts. It shows that with increasing La content in the catalyst, the selectivity to VF is enhanced from 66.3 to 88.3%, while the selectivity to HFC-152a decreases from 32.3 to 9.6%. Also, the coke formation is slightly suppressed by the La addition. These results (Tables 2 and 3) indicate that the addition of a small amount of La into the Al_2O_3 catalyst can not only keep high C_2H_2 conversion but also enhance the VF selectivity and reduce the coke deposition.

2.3. Catalytic stability of Al_2O_3 and $La_2O_3(1)-Al_2O_3$ catalysts

Fig. 2 shows the catalytic performances of the pure Al_2O_3 and the $La_2O_3(1)-Al_2O_3$ catalysts as a function of reaction time. For the Al_2O_3 catalyst, as can be seen in Fig. 2(a), the C_2H_2 conversion slightly decreases from the initial value of 96.1% to the final value of 90.8% during the reaction time of 100 h and has a decreasing tendency, while the selectivities to VF and HFC-152a have no big undulation. The selectivity to coke deposition is about 2.1% at the beginning and drops to 1.8% after 70 h reaction. For the $La_2O_3(1)-Al_2O_3$ catalyst, as shown in Fig. 2(b), the C_2H_2 conversion keeps constant (ca. 95.0%) in a time course of 100 h. The selectivity to VF shows a gentle increase from 81.5 to 85.8%, while those to coke deposition and HFC-152a decline gently.

Table 3

Influence of La content on the products selectivities at the 90% of C_2H_2 conversion over $La_2O_3-Al_2O_3$ catalysts.

La content (mol%)	Selectivity (%)		
	VF	HFC-152a	Coke deposition
0	66.3	32.2	1.2
1	75.0	23.4	0.8
5	75.1	23.5	0.8
10	88.3	9.6	0.9

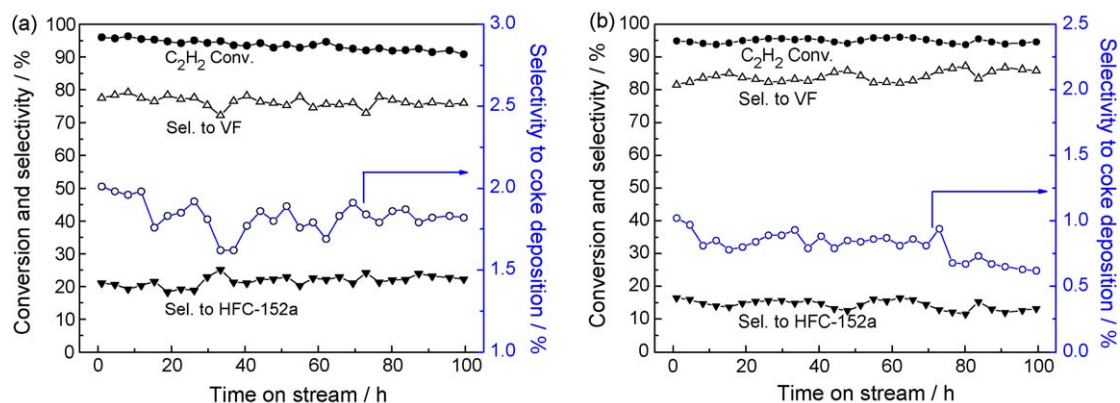


Fig. 2. C_2H_2 conversion, main products selectivities and coke deposition selectivity at 300 °C on (a) Al_2O_3 and (b) $La_2O_3(1)-Al_2O_3$ catalysts with time on stream.

Comparing these two catalysts, it can be concluded that the initial activity of Al_2O_3 catalyst is high, but it decreases with time on stream. The selectivity to the desired product VF on $La_2O_3(1)-Al_2O_3$ catalyst is higher than pure Al_2O_3 catalyst. The selectivity to coke deposition on the pure Al_2O_3 catalyst is much higher than that on the $La_2O_3(1)-Al_2O_3$ catalyst. The difference in catalytic behaviors between these two catalysts indicates that the addition of La may change the surface property of the catalyst, thus alter the reaction procedures for the formation of VF, HFC-152a and coke deposition.

2.4. Characterizations

Table 4 lists the properties of the fresh, pre-fluorinated and used $La_2O_3-Al_2O_3$ catalysts. It is found that surface areas of the fresh catalysts decrease dramatically with increasing La content, while those of the pre-fluorinated and used catalysts are not greatly affected. Compared with the fresh catalyst, the surface areas of the pre-fluorinated and used catalysts are much smaller. This may be due to the formation of AlF_3 and LaF_3 during the pre-fluorination process, which has much lower surface area than the corresponding oxide. Also, there is no obvious change in the surface areas of the pre-fluorinated and used catalysts, indicating that the coke deposited on the catalyst surface barely affects the surface areas of these catalysts, and the slight deviation in the BET surface areas is probably due to the error caused by the method of measurement. Considering the crystallite size of the catalyst, it is found that the crystallite size of the pre-fluorinated $La_2O_3-Al_2O_3$ catalysts range from 3.3 to 3.5 nm, implying that these samples are nano-sized materials.

The XRD patterns of the fresh, pre-fluorinated and used $La_2O_3-Al_2O_3$ catalysts are given in Fig. 3. For the fresh catalysts, as can be seen in Fig. 3(a), the diffraction peaks at 22.8, 26.6, 40.1 and 44.7° can be attributed to La_2O_3 [15, JCPDS card 83-1355] and these peaks become sharper with increasing La content whereas diffraction peaks assigned to Al_2O_3 become weaker correspondingly. Also, a solid solution phase ascribed to perovskite crystal

structural $LaAlO_3$ [24] emerges. This indicates that the La_2O_3 accumulates on the catalyst surface when its content is high. For the pre-fluorinated catalysts, Fig. 3(b) shows the distinct evolution of AlF_3 and LaF_3 phases. For the used catalysts (after 8 h reaction),

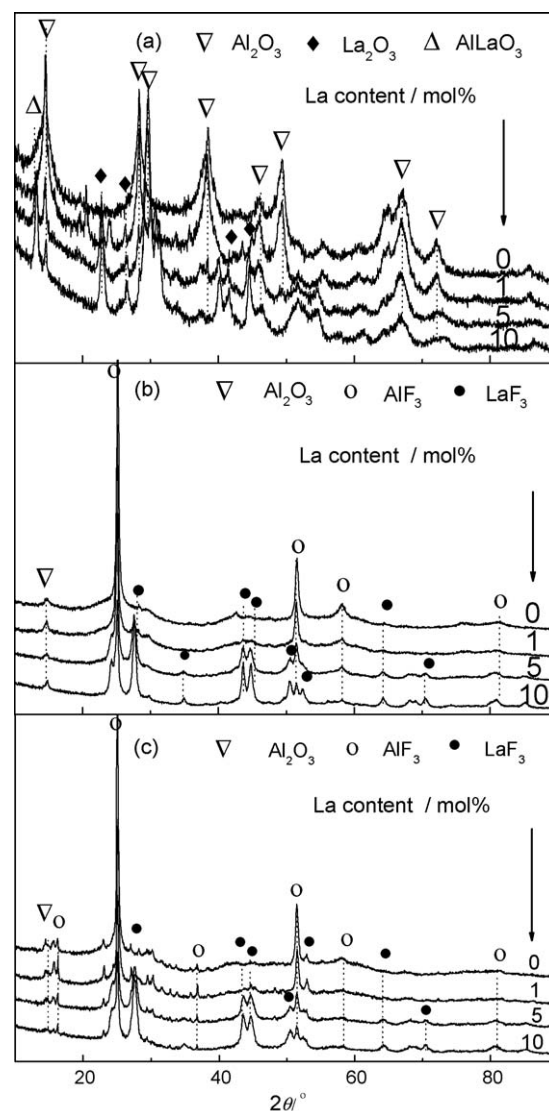


Fig. 3. XRD patterns of (a) fresh, (b) pre-fluorinated and (c) used $La_2O_3-Al_2O_3$ catalysts.

Table 4
Properties of fresh, pre-fluorinated and used $La_2O_3-Al_2O_3$ catalysts.

La content (mol%)	BET surface area ($m^2 g^{-1}$)			Crystallite size of pre-fluorinated catalysts (nm)
	Fresh catalysts	Pre-fluorinated catalysts	Used catalysts	
0	282	32	36	3.3
1	240	30	37	3.3
5	199	30	33	3.5
10	169	29	29	3.4

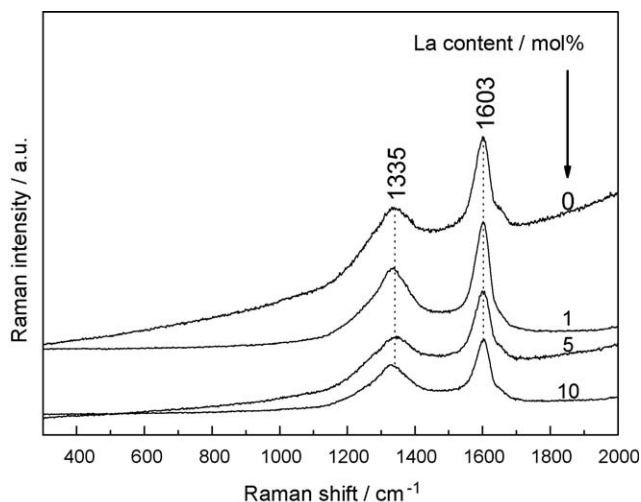


Fig. 4. Raman spectra of used $\text{La}_2\text{O}_3\text{-Al}_2\text{O}_3$ catalysts.

Fig. 3(c) clearly shows that the diffraction features of the used catalysts are almost identical to the corresponding pre-fluorinated catalysts. These results indicate that the LaAlO_3 and La_2O_3 have almost completely converted to AlF_3 and LaF_3 in the pre-fluorination process. However, there is still a weak peak at 14.6° ascribed to Al_2O_3 , implying that the phase transition of Al_2O_3 is somehow incomplete. The XRD results could explain well the decline in the surface areas of the pre-fluorinated catalysts, due to the phase transition of La_2O_3 and Al_2O_3 to LaF_3 and AlF_3 , respectively.

Fig. 4 shows the Raman spectra of the used $\text{La}_2\text{O}_3\text{-Al}_2\text{O}_3$ catalysts. A band at 1335 cm^{-1} can be attributed to the C–H distortion vibration peak and a band at 1603 cm^{-1} to the C=C expansion vibration peak, which are both due to Raman vibration of coke deposition [25]. These two peaks become weaker with increasing La content in the catalyst, indicating that the amount of coke deposition on the catalyst surface reduces. This result is in good agreement with the results listed in Table 2. But there are no Raman characteristic peaks for Al and La oxide compounds or their fluorides, which may be related either to the strong fluorescent effect of Al and La or to the carbon deposition that may cover their oxide or fluoride compounds.

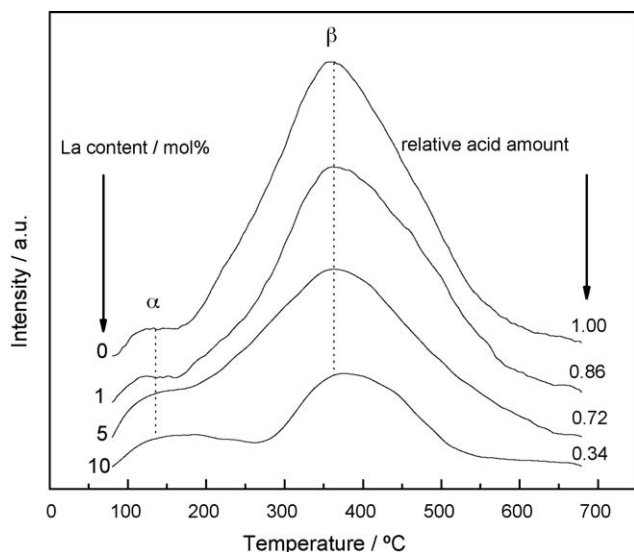


Fig. 5. NH_3 -TPD profiles of pre-fluorinated $\text{La}_2\text{O}_3\text{-Al}_2\text{O}_3$ catalysts.

NH_3 -TPD experiments were performed in order to obtain information of the acidity of these catalysts. Fig. 5 presents the desorption traces for the pre-fluorinated $\text{La}_2\text{O}_3\text{-Al}_2\text{O}_3$ catalysts. A typical profile shows that there is a desorption peak α at 135°C and a peak β at 363°C , the latter of which is wider and bigger. The peak α can be ascribed to the NH_3 adsorbed on the weak acidic sites and the peak β to the NH_3 adsorbed on the strong acidic sites [26]. The peak position does not shift with increasing La content, indicating that the nature of acid centers keeps unchanged. But the area of the peak β decreases with increasing La content in the catalyst, implying a decline in the total amount of the strong surface acidic sites.

Nano-sized AlF_3 is known to be one of the most effective solid Lewis acids [27–30]. In contrast, LaF_3 is slightly alkalescent. The amount of surface acidic sites could be calculated based on the relative proportion of the peak area. Relative amount of acidic sites on these pre-fluorinated $\text{La}_2\text{O}_3\text{-Al}_2\text{O}_3$ catalysts drops from 1.00 to 0.34 as the content of La increases from 0 to 10 mol. %. The decline could be attributed to the fact that LaF_3 species cover some surface acidic sites provided by AlF_3 , or the relative content of AlF_3 reduces in the La-rich catalyst, as in the pre-fluorinated $\text{La}_2\text{O}_3(10)\text{-Al}_2\text{O}_3$ catalyst.

In order to determine the nature of acidic sites, pyridine adsorption experiments were performed. Fig. 6 shows the IR spectra of adsorbed pyridine on pre-fluorinated $\text{La}_2\text{O}_3\text{-Al}_2\text{O}_3$ catalysts. Several feature bands are observed at 1454 , 1490 , 1540 and 1625 cm^{-1} on these samples, and their intensities become weaker with increasing La content in the catalysts. The bands at 1450 , 1490 and 1620 cm^{-1} could be attributed to pyridine adsorbed on Lewis acidic sites; while the band at 1540 cm^{-1} could be attributed to pyridine adsorbed on Brønsted acidic sites [31,32]. The IR results indicate that the surface of the pre-fluorinated $\text{La}_2\text{O}_3\text{-Al}_2\text{O}_3$ catalysts mainly consist of Lewis acidic sites. Furthermore, the relative amount of these sites declines with increasing La content in the catalysts, which is in agreement with the NH_3 -TPD experiments (Fig. 5).

In the current study, the crystallite size of obtained pre-fluorinated $\text{La}_2\text{O}_3\text{-Al}_2\text{O}_3$ catalysts are nano-scaled (Table 4). Therefore, they can provide sufficient Lewis acidic sites, as shown in Fig. 6. The catalytic properties of the $\text{La}_2\text{O}_3\text{-Al}_2\text{O}_3$ catalysts are closely related to the surface acidity, since the adsorption of

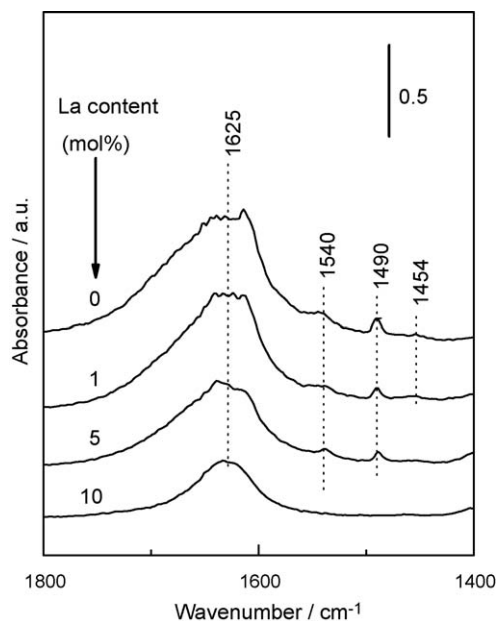


Fig. 6. IR spectra of pyridine adsorption on pre-fluorinated $\text{La}_2\text{O}_3\text{-Al}_2\text{O}_3$ catalysts.

organic substances (including acetylene) mainly occurs on the surface acidic sites of the catalyst [7]. A high surface density of acidic sites will certainly enhance the initial reactivity, however, the enhancement in reactivity also results in the accelerated consecutive reaction between the VF and HF to further produce HFC-152a, as well as the coke deposition, as can be seen in the case of pure Al_2O_3 (Tables 2 and 3 and Fig. 2). For the La-doped Al_2O_3 catalyst, although the initial reactivity is suppressed due to the decline in surface density of acidic sites, the consecutive reaction of VF with HF, and the coke deposition are also inhibited. This could explain the enhancement in the selectivity to the desired VF and the drop in the selectivities to the by-product HFC-152a and coke deposition.

3. Conclusions

A series of La_2O_3 - Al_2O_3 catalysts with different La contents were prepared and tested for vapor phase hydrofluorination of C_2H_2 to VF. The high activity to C_2H_2 and high selectivity to VF was obtained over a pre-fluorinated $\text{La}_2\text{O}_3(1)$ - Al_2O_3 catalyst, detailed with 94.5% of C_2H_2 conversion and 84.1% of VF selectivity and only 0.9% of coke deposition selectivity at 300 °C, with a HF/ C_2H_2 molar ratio of 2.5. Furthermore, this catalyst gave a better stability compared with the pure Al_2O_3 . LaF_3 played an important role in the catalytic performance by modifying the surface acidic property of the catalyst, which led to a considerable enhancement of selectivity to VF and a slight decline in C_2H_2 conversion over the La-doped Al_2O_3 catalyst.

4. Experimental

4.1. Catalyst preparation

The La_2O_3 - Al_2O_3 catalysts were prepared using a deposition-precipitation (DP) method. A detailed process is as follows: an aqueous solution of $\text{La}(\text{NO}_3)_3$ was mixed with a $\text{Al}_2\text{O}_3 \cdot \text{H}_2\text{O}$ powder at room temperature, then an aqueous solution of $(\text{NH}_4)_2\text{CO}_3$ (1 M) was added drop-wise to the mixture under stirring until the pH was brought to about 8.0. The resulting mixture was aged for 1 h and then the solid was separated from the mother liquid. It was washed with deionized water and dried at 120 °C overnight, followed by a calcination at 400 °C for 4 h. The La contents in the catalysts were 0, 1, 5 and 10 mol.%, and the catalysts were denoted as Al_2O_3 , $\text{La}_2\text{O}_3(1)$ - Al_2O_3 , $\text{La}_2\text{O}_3(5)$ - Al_2O_3 and $\text{La}_2\text{O}_3(10)$ - Al_2O_3 , with the number in the parenthesis representing the La content in the catalyst.

4.2. Catalyst characterizations

Surface areas of the catalysts were determined by the modified BET method from the N_2 sorption isotherms at 77 K on an Auto-sorb-1 apparatus.

X-ray diffraction (XRD) patterns were collected on a PANalytical X'Pert PROMPD powder diffractometer operated at 40 kV and 40 mA, using $\text{Cu K}\alpha$ radiation. The catalyst was scanned in a 2θ range from 10 to 90° with a scan rate of $0.3^\circ \text{ min}^{-1}$. The phase compositions of the catalysts were identified with reference to the power diffraction data files (JCPDS). The crystallite size of pre-fluorinated samples was calculated by full curve fitting, using Jade 6.5 software.

Raman spectra were obtained on a Renishaw RM1000 confocal microscope with exciting wavelength of 514.5 nm under ambient conditions, which were used to get the information of coke deposition over the used catalysts.

Temperature-programmed desorption of ammonia (NH_3 -TPD) was employed to determine the strength of acidic sites and its distribution of the pre-fluorinated catalysts. The sample (0.1 g) was

first heated up to 550 °C and kept for 30 min in flow of Ar (30 mL min^{-1}), then it was cooled down to 80 °C. A flow of NH_3 (20 mL min^{-1}) was then introduced for 60 min. The gaseous or physisorbed NH_3 was removed by Ar flow (30 mL min^{-1}) at 80 °C for 1 h, then the sample was heated to 680 °C with a ramp of $10^\circ \text{ C min}^{-1}$. The desorbed NH_3 was monitored continuously via a TCD detector.

The FTIR spectra of pyridine adsorption on the pre-fluorinated catalysts were recorded on a Nicolet NEXUS 670 spectrometer in the range 1800 – 1400 cm^{-1} . The pre-fluorinated catalysts were dried in a hot air oven for 1 h at 100 °C prior to pyridine treatment. A self-supported pellet of catalyst was brought in contact with pyridine directly. Then the sample was kept in a hot air oven at 120 °C for 1 h to remove physisorbed pyridine. After cooling the catalyst sample to room temperature, the IR spectrum was recorded in the spectral range 1800 – 1400 cm^{-1} with 256 scans and at a resolution of 4 cm^{-1} using KBr background at room temperature.

4.3. Catalyst activation (pre-fluorination)

Prior to use, the fresh catalyst was subject to a pre-fluorination process in order to activate the catalyst. The pre-fluorination was carried out in a stainless steel tubular reactor with an inner diameter of 1 cm and a length of 30 cm. 3 mL of the fresh catalyst (20–40 mesh) was loaded in the reactor and dried at 300 °C for 1 h in N_2 (30 mL min^{-1}). Then the N_2 flow was stopped and a mixture of HF (80 mL min^{-1}) and N_2 (10 mL min^{-1}) was introduced at 260 °C for 1.5 h and subsequently at 350 °C for 2 h. The fresh catalyst after the activation process was denoted as the pre-fluorinated catalyst.

4.4. Hydrofluorination reaction

The hydrofluorination reactions were carried out in the same reactor soon after the catalyst activation, under atmospheric pressure. 3 mL of the in situ pre-fluorinated catalyst was used. Flow rates of C_2H_2 and HF gases were carefully controlled using mass flow controllers. The molar ratio of HF/ C_2H_2 was 2.5 and the GHSV was 900 h^{-1} . The gaseous products were analyzed by a gas chromatograph (Shimadzu GC-2014) equipped with a flame ionization detector (FID) and a HP GS-GASPRO capillary column. After hydrofluorination reaction, the catalyst was denoted as the used catalyst.

4.5. Coke deposition calculation

In vapor phase hydrofluorination of C_2H_2 to VF, a small quantity of C_2H_2 could be decomposed into carbon and ethylene (reaction (5)), and this ethylene could also react with HF to produce $\text{CH}_3\text{CH}_2\text{F}$ (reaction (6)).



Furthermore, the deposited coke species include mostly carbon and small amount of polymerized C_2H_2 and other unsaturated hydrocarbons. So the selectivity to coke deposition could be calculated as follows:

$$[\text{Selectivity to coke deposition}] = 2 \times ([\text{Selectivity to } \text{C}_2\text{H}_4] + [\text{Selectivity to } \text{CH}_3\text{CH}_2\text{F}])$$

Acknowledgements

This work is financially supported by the National Science Foundation of China (Grant No. 20873125). The authors are also

grateful to Prof. Zhao-Yin Hou from the Institute of Catalysis, Zhejiang University, for the NH₃–TPD analysis.

References

- [1] D. Sianesi, G. Nelli, *Chimica*, US Patent 3,200,160 (1965).
- [2] J.W.H. Tustin, *Calif*, US Patent 3,621,067 (1971).
- [3] T.E. Hedge, Wickliffe, D.F. Cooley, C.E. Entemann, Painesville, R. Steinkoenig, Chardon, R.L. Urbanowski, US Patent 3,317,619 (1967).
- [4] B.F. Skiles, *Wilmington*, US Patent 2,892,000 (1959).
- [5] E.H. Lee, *Catal. Rev. Sci. Eng.* 8 (1973) 285.
- [6] M.S. Ramos, M.S. Santos, L.P. Gomes, A. Alborno, M.C. Rangel, *Appl. Catal. A* 341 (2008) 12–17.
- [7] O. Macias, J. Largo, C. Pesquera, C. Blanco, F. González, *Appl. Catal. A* 314 (2006) 23–31.
- [8] R.M. Navarro, M.C. Álvarez-Galván, F. Rosa, J.L.G. Fierro, *Appl. Catal. A* 297 (2006) 60–72.
- [9] A. Parmaliana, F. Arena, F. Frusteri, S. Coluccia, L. Marchese, G. Martra, A.L. Chuvilin, *J. Catal.* 141 (1993) 34–47.
- [10] V.R. Choudhary, B.S. Uphade, A.S. Mamman, *Catal. Lett.* 32 (1995) 387–390.
- [11] T. Oxaki, T. Mori, *J. Catal.* 204 (2001) 89–97.
- [12] D.L. Trimm, *Catal. Today* 49 (1999) 3–10.
- [13] R. Martínez, E. Romero, C. Guimon, R. Bilbao, *Appl. Catal. A* 274 (2004) 139–149.
- [14] B.S. Liu, C.T. Au, *Appl. Catal. A* 244 (2003) 181–195.
- [15] F.X. Yin, S.F. Ji, B.H. Chen, Z.L. Zhou, H. Liu, C.Y. Li, *Appl. Catal. A* 310 (2006) 164–173.
- [16] P. Budi, E. Curry-Hyde, R.F. Howe, *Catal. Lett.* 41 (1996) 47–53.
- [17] E. Arendt, A. Maione, A. Klisinska, O. Sanz, M. Montes, S. Suarez, J. Blanco, P. Ruiz, *Appl. Catal. A* 339 (2008) 1–14.
- [18] S. Cimino, L. Lisi, R. Pirone, G. Russo, M. Turco, *Catal. Today* 59 (2000) 19–31.
- [19] L. Znak, K. Stolecki, J. Zielinski, *Catal. Today* 101 (2005) 65–71.
- [20] R. Burch, P.J.F. Harris, C. Pipe, *Appl. Catal. A* 210 (2001) 63–73.
- [21] B. Białobok, J. Trawczyński, W. Miśta, M. Zawadzki, *Appl. Catal. B* 72 (2007) 395–403.
- [22] L.J. Kundakovic, M. Flytzani-Stephanopoulos, *J. Catal.* 179 (1998) 203–221.
- [23] J.C.S. Araujo, D. Zanchet, R. Rinaldi, U. Schuchardt, C.E. Hori, J.L.G. Fierro, J.M.C. Bueno, *Appl. Catal. B* 84 (2008) 552–562.
- [24] J.W. Fergus, *J. Fluorine Chem.* 78 (1996) 83–86.
- [25] C. Li, P.C. Stair, *Stud. Sci. Catal.* 101 (1996) 881–890.
- [26] K. Scheurell, G. Scholz, A. Pawlik, E. Kemnitz, *Solid State Sci.* 10 (2008) 873–883.
- [27] M. Nickkho-Amiry, G. Eltanany, S. Wuttke, S. Rüdiger, E. Kemnitz, J.M. Winfield, *J. Fluorine Chem.* 129 (2008) 366–375.
- [28] E. Kemnitz, U. Groß, St. Rüdiger, S.C. Shakar, *Angew. Chem., Int. Ed.* 42 (2003) 4251–4254.
- [29] St.K. Rüdiger, U. Groß, M. Feist, H.A. Prescott, S.C. Shakar, S.I. Troyanov, E. Kemnitz, *J. Mater. Chem.* 15 (2005) 588–597.
- [30] St. Rüdiger, U. Groß, E. Kemnitz, *J. Fluorine Chem.* 128 (2007) 353–368.
- [31] C.R. Reddy, Y.S. Bhat, G. Nagendrappa, B.S.J. Prakash, *Catal. Today* 141 (2009) 157–160.
- [32] L. Jankovič, P. Komadel, *J. Catal.* 218 (2003) 227–233.